

A Design and an Implementation of an Inverse Kinematics Computation in Robotics Using Real Quantifier Elimination based on Comprehensive Gröbner Systems

Shuto Otaki, Akira Terui and Masahiko Mikawa

Abstract. The solution and implementation of the inverse kinematics computation of a three degree-of-freedom (DOF) robot manipulator using an algorithm for real quantifier elimination with Comprehensive Gröbner Systems (CGS) are presented. The method enables us to verify if the given parameters are feasible before solving the inverse kinematics problem. Furthermore, pre-computation of CGS and substituting parameters in the CGS with the given values avoids the repetitive computation of the Gröbner basis. Experimental results compared with our previous implementation are shown.

Mathematics Subject Classification (2010). 68W30, 13P10, 13P25.

Keywords. Comprehensive Gröbner Systems, Quantifier elimination, Robotics, Inverse kinematics.

1. Introduction

1.1. The inverse kinematic problem

In this paper, we discuss solving the inverse kinematic problem in motion planning in robotics [23] with computer algebra. In motion planning of a robot such as a manipulator with joints connected with links consecutively, we consider the forward and the inverse kinematic problems. While the forward kinematic problem is to determine the position of the end-effector for the given configuration (angles) of the joints, the inverse kinematic problem is to determine the configuration of the joints to bring the end-effector to the desired position. For the given position of the end-effector, one solves the inverse kinematic problem to obtain the configuration of the joints. For solving

the inverse kinematic problem, the forward kinematic problem is formulated, then the inverse kinematic problem is derived.

Among various methods for inverse kinematics computation, methods using Gröbner bases have been proposed ([6, 9, 27, 28], and the references therein). In these methods, the inverse kinematics problem is expressed as a system of polynomial equations with trigonometric functions substituted with variables, along with polynomial constraints defining the relationship of these new variables. Then, the system of equations is triangularized by computing the Gröbner basis with respect to the lexicographic ordering and solved by appropriate solvers. An advantage of the methods using Gröbner bases is that, since they solve the inverse kinematic problem directly, one can verify if there exists a real solution of the inverse kinematic problem and if there exists a real solution, one can obtain the configuration of the joints prior to the actual motion. On the other hand, the computing time of Gröbner bases may affect the computational cost of the methods: thus, it is desirable to decrease computational cost for computing Gröbner bases and related computations.

1.2. Our previous work

Two of the present authors have proposed the implementation of inverse kinematics computation of a three degree-of-freedom (DOF) robot manipulator using Gröbner bases [8]. The implementation uses SymPy [14], a library for computer algebra written in Python, with the computer algebra system Risa/Asir [18, 19], connected with OpenXM infrastructure for communicating mathematical software systems [13, 20].

We have made our implementation in this way with the following intentions. The first was for building an inverse kinematic solver with free software that is easily integrated with robotics middleware such as the Robot Operating System (ROS) [12]. While some inverse kinematics solvers in computer algebra have been proposed using commercial computer algebra systems [2, 11, 17, 22, 31], in the robotics community, much software packages are developed as free and open-source software, including ROS. Also, Python is frequently used in robotics and can easily be integrated with ROS. Thus, we claim that one can easily incorporate our implementation with ROS or other software related to robotics. Furthermore, for efficient computation of Gröbner bases with a computer algebra system which can be called easily from Python and distributed as free software, we have employed Risa/Asir for that purpose.

Another one was choosing an appropriate solver for solving a system of polynomial equations among those available in Python's various packages.

However, our implementation had its challenges: one was that we were solving inverse kinematic problems without verifying the existence of a real solution. Another one was the computation of Gröbner basis every time in solving the inverse kinematic problem. It would be better to avoid repetitive computation of Gröbner basis if we repeat the inverse kinematics computation

many times; otherwise, it may make the whole computation inefficient for large-scale problems such as ones with many degrees of freedom.

1.3. Aim of the present paper

In this paper, we overcome these challenges by using an algorithm for real quantifier elimination based on Comprehensive Gröbner Systems (CGS) [10, 15, 25], known as the CGS-QE algorithm, which was initially proposed by Weispfenning [32] and improved by Fukasaku et al. [7]. The inverse kinematic problem is expressed as a system of polynomial equations with the coordinates of the end-effector expressed as parameters. Then, with the CGS-QE algorithm, the existence of real roots of the polynomial system is verified for the given coordinates. Furthermore, by solving the system of polynomial equations defined as the CGS with the parameters substituted with the given coordinates, the roots of the inverse kinematic problem are computed without repeated computation of Gröbner bases. Note that, although in the *preprocessing steps* (see Section 4) prior to solving inverse kinematic problems, Wolfram Mathematica is used for simplification of formulas, the *main steps* for solving inverse kinematic problem is carried out with Python and Risa/Asir for our intention of using free software.

1.4. Plan for the paper

This paper is organized as follows. In Section 2, we formulate the inverse kinematics problem of a 3 DOF manipulator for solving it using Gröbner bases. In Section 3, we review a part of the CGS-QE algorithm including the definition of the CGS and the theory of real root counting. In Section 4, we present our method of solving the inverse kinematic problem using the CGS-QE algorithm. In Section 6, we present the result of the experiments. Note that our implementation and the result of the experiments are freely available [26]. Finally, in Section 7, conclusions and future research direction are presented.

2. Inverse kinematics of a 3 DOF robot manipulator

In this paper, we consider an inverse kinematic problem of a 3 DOF robot manipulator build with LEGO[®] MINDSTORMS[®] EV3 Education¹ (henceforth abbreviated to EV3) (Figure 1). It has a set of servo motors and sensors (gyro, ultrasonic, color, and touch sensors) controlled by a computer (called “EV3 Intelligent Brick”). One can build a manipulator (or other kinds of robots) using bricks with these components, and control its motion using either a GUI-based programming environment that is officially available or a programming language from those including Python, Ruby, C, and Java.

The components of the manipulator are shown as in Figure 2². Links

¹LEGO and MINDSTORMS are trademarks of the LEGO Group.

²While the manipulator itself is the same one used in our previous paper [8], we have re-measured the structure of joints and links; thus, the derived inverse kinematic problem in the present paper is slightly different from the one in the previous paper.

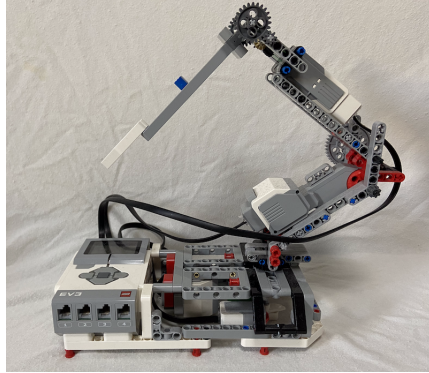


FIGURE 1. A 3 DOF manipulator built with EV3.

are called Link i ($i = 0, \dots, 7$) from the one fixed on the ground towards the end-effector. For $j = 1, \dots, 7$, a joint connecting Link $j - 1$ and j is called Joint j . Note that Joints 1, 4, 7 are revolute joints, while the other joints are fixed, and all the joints and links are located on a plane. Among Joints 1, 4, 7, Joint 1 has a diamond shape because the axis of rotation overlaps with Links 0 and 1, while Joints 4 and 7 are drawn in a circle because the axis of rotation is perpendicular to the links connected to the joint.

For Joint j with $j = 1, \dots, 7$, the coordinate system Σ_j , with the x_j , y_j and z_j axes and the origin at Joint j , is defined according to a modified Denavit–Hartenberg convention [30] (Figure 2), as follows.

- The z_j axis is chosen along with the axis of Joint j .
- The x_{j-1} axis is chosen along with with the common normal to axes z_{j-1} to z_j .
- The y_j axis is chosen so that the present coordinate system is right-handed.

Note that, since the present coordinate system is right-handed, the positive axis pointing upwards and downwards are denoted by “ \odot ” and “ \otimes ”, respectively. Now, let us regard the perpendicular foot on the ground from Joint 1 as Joint 0 and let Σ_0 be the coordinate system with the origin placed at the position of Joint 0, where the direction of axes x_0 , y_0 , and z_0 are the same as that of axes x_1 , y_1 and z_1 , respectively. Also, let us regard the end-effector as Joint 8 and let Σ_8 be the coordinate system with the origin placed at the position of Joint 8, where the direction of axes x_8 , y_8 , and z_8 are the same as that of axes x_7 , y_7 , and z_7 , respectively.

For analyzing the motion of the manipulator, we define a map between the *joint space* and the *configuration space* or *operational space*. For a joint space, since we have revolute joints 1, 4, 7, their angles $\theta_1, \theta_4, \theta_7$, respectively, are located in a circle S^1 , we define the joint space as $\mathcal{J} = S^1 \times S^1 \times S^1$. For a configuration space, let (x, y, z) be the position of the end-effector located in \mathbb{R}^3 and then define the configuration space as $\mathcal{C} = \mathbb{R}^3$. Thus, we consider

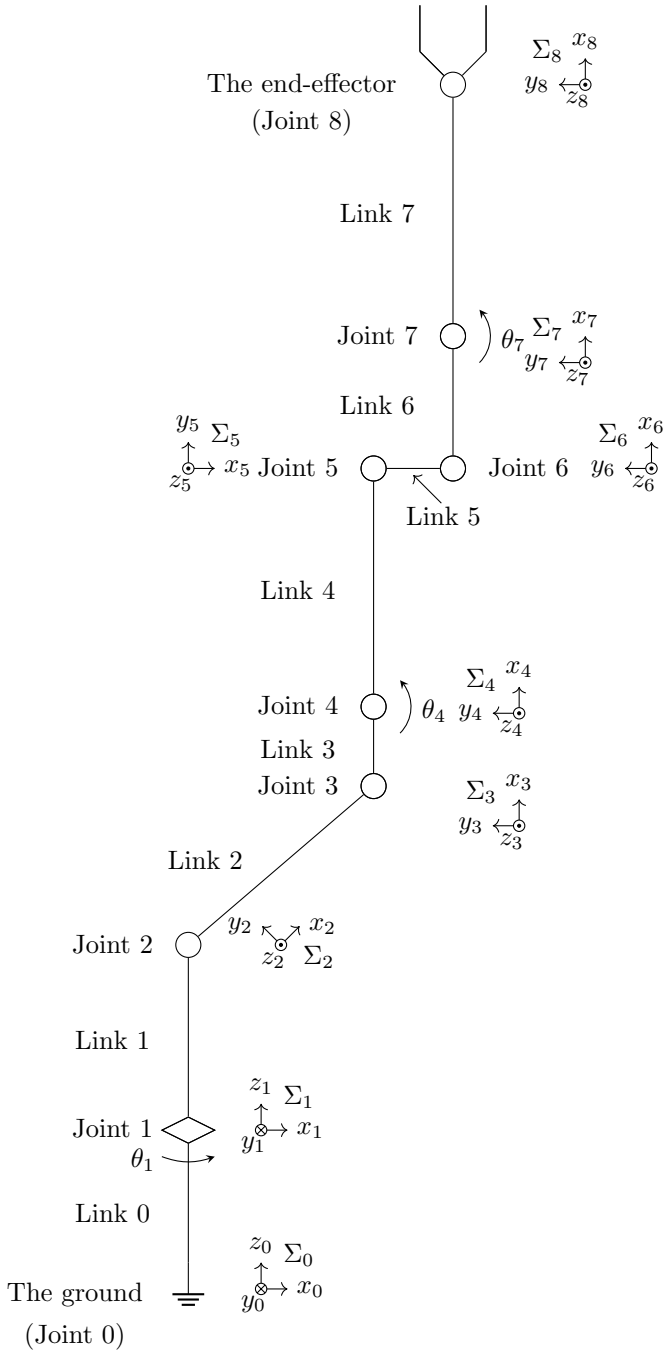


FIGURE 2. Components and the coordinate systems of the manipulator.

TABLE 1. Joint parameters for EV3.

j	a_j (mm)	α_j	d_j (mm)	θ_j
1	0	0	80	θ_1
2	0	$\pi/2$	0	$\pi/4$
3	88	0	0	$\pi/4$
4	24	0	0	θ_4
5	96	0	0	$-\pi/2$
6	16	0	0	$\pi/2$
7	40	0	0	θ_7
8	112	0	0	0

a map $f : \mathcal{J} \rightarrow \mathcal{C}$. The forward kinematic problem is to find the position of the end-effector in \mathcal{C} for the given configuration of the joints in \mathcal{J} , while the inverse kinematic problem is to find the configuration of the joints in \mathcal{J} which enables the given position of the end-effector in \mathcal{C} . We first solve the forward kinematic problem for formulating the inverse kinematic problem.

Let a_j be the length of the common perpendicular line segment of axes z_{j-1} and z_j , α_j the angle between axes z_{j-1} and z_j with respect to the x_{j-1} axis, d_j the length of the common perpendicular line segment of axes x_{j-1} and x_j , and θ_j be the angle between axes x_{j-1} and x_j with respect to z_j axis. Then, the coordinate transformation matrix ${}^{j-1}T_j$ from the coordinate system Σ_i to Σ_{j-1} is expressed as

$$\begin{aligned}
{}^{i-1}T_i &= \begin{pmatrix} 1 & 0 & 0 & a_j \\ 0 & 1 & 0 & 0 \\ 0 & 0 & 1 & 0 \\ 0 & 0 & 0 & 1 \end{pmatrix} \times \begin{pmatrix} 1 & 0 & 0 & 0 \\ 0 & \cos \alpha_j & -\sin \alpha_j & 0 \\ 0 & \sin \alpha_j & \cos \alpha_j & 0 \\ 0 & 0 & 0 & 1 \end{pmatrix} \\
&\times \begin{pmatrix} 1 & 0 & 0 & 0 \\ 0 & 1 & 0 & 0 \\ 0 & 0 & 1 & d_j \\ 0 & 0 & 0 & 1 \end{pmatrix} \times \begin{pmatrix} \cos \theta_j & -\sin \theta_j & 0 & 0 \\ \sin \theta_j & \cos \theta_j & 0 & 0 \\ 0 & 0 & 1 & 0 \\ 0 & 0 & 0 & 1 \end{pmatrix} \\
&= \begin{pmatrix} \cos \theta_j & -\sin \theta_j & 0 & a_j \\ \cos \alpha_j \sin \theta_j & \cos \alpha_j \cos \theta_j & -\sin \alpha_j & -d_j \sin \alpha_j \\ \sin \alpha_j \sin \theta_j & \sin \alpha_j \cos \theta_j & \cos \alpha_j & d_j \cos \alpha_j \\ 0 & 0 & 0 & 1 \end{pmatrix},
\end{aligned}$$

where the joint parameters a_j , α_j , d_j and θ_j are given as shown in Table 1 (note that the unit of a_j and d_j is millimeters). The transformation matrix T from the coordinate system Σ_8 to Σ_0 is calculated as $T =$

${}^0T_1{}^1T_2{}^2T_3{}^3T_4{}^4T_5{}^5T_6{}^6T_7{}^7T_8$, where

$$\begin{aligned}
 {}^0T_1 &= \begin{pmatrix} \cos \theta_1 & -\sin \theta_1 & 0 & 0 \\ \sin \theta_1 & \cos \theta_1 & 0 & 0 \\ 0 & 0 & 1 & 80 \\ 0 & 0 & 0 & 1 \end{pmatrix}, & {}^1T_2 &= \begin{pmatrix} \frac{\sqrt{2}}{2} & -\frac{\sqrt{2}}{2} & 0 & 0 \\ 0 & 0 & -1 & 0 \\ \frac{\sqrt{2}}{2} & \frac{\sqrt{2}}{2} & 0 & 0 \\ 0 & 0 & 0 & 1 \end{pmatrix}, \\
 {}^2T_3 &= \begin{pmatrix} \frac{\sqrt{2}}{2} & -\frac{\sqrt{2}}{2} & 0 & 88 \\ \frac{\sqrt{2}}{2} & \frac{\sqrt{2}}{2} & 0 & 0 \\ 0 & 0 & 1 & 0 \\ 0 & 0 & 0 & 1 \end{pmatrix}, & {}^3T_4 &= \begin{pmatrix} \cos \theta_4 & -\sin \theta_4 & 0 & 24 \\ \sin \theta_4 & \cos \theta_4 & 0 & 0 \\ 0 & 0 & 1 & 0 \\ 0 & 0 & 0 & 1 \end{pmatrix}, \\
 {}^4T_5 &= \begin{pmatrix} 0 & 1 & 0 & 96 \\ -1 & 0 & 0 & 0 \\ 0 & 0 & 1 & 0 \\ 0 & 0 & 0 & 1 \end{pmatrix}, & {}^5T_6 &= \begin{pmatrix} 0 & -1 & 0 & 16 \\ 1 & 0 & 0 & 0 \\ 0 & 0 & 1 & 0 \\ 0 & 0 & 0 & 1 \end{pmatrix}, \\
 {}^6T_7 &= \begin{pmatrix} \cos \theta_7 & -\sin \theta_7 & 0 & 40 \\ \sin \theta_7 & \cos \theta_7 & 0 & 0 \\ 0 & 0 & 1 & 0 \\ 0 & 0 & 0 & 1 \end{pmatrix}, & {}^7T_8 &= \begin{pmatrix} 1 & 0 & 0 & 112 \\ 0 & 1 & 0 & 0 \\ 0 & 0 & 1 & 0 \\ 0 & 0 & 0 & 1 \end{pmatrix}. \tag{1}
 \end{aligned}$$

Then, the position (x, y, z) of the end-effector with respect to the coordinate system Σ_0 is expressed as

$$\begin{aligned}
 x &= -112 \cos \theta_1 \cos \theta_4 \sin \theta_7 + 16 \cos \theta_1 \cos \theta_4 - 112 \cos \theta_1 \sin \theta_4 \cos \theta_7 \\
 &\quad - 136 \cos \theta_1 \sin \theta_4 + 44\sqrt{2} \cos \theta_1, \\
 y &= -112 \sin \theta_1 \cos \theta_4 \sin \theta_7 + 16 \sin \theta_1 \cos \theta_4 - 112 \sin \theta_1 \sin \theta_4 \cos \theta_7 \\
 &\quad - 136 \sin \theta_1 \sin \theta_4 + 44\sqrt{2} \sin \theta_1, \\
 z &= 112 \cos \theta_4 \cos \theta_7 + 136 \cos \theta_4 - 112 \sin \theta_4 \sin \theta_7 + 16 \sin \theta_4 \\
 &\quad + 104 + 44\sqrt{2}. \tag{2}
 \end{aligned}$$

The inverse kinematic problem is solving Equation (2) with respect to $\theta_1, \theta_4, \theta_7$. By substituting trigonometric functions $\cos \theta_j$ and $\sin \theta_j$ with variables as

$$c_j = \cos \theta_j, \quad s_j = \sin \theta_j,$$

subject to $c_j^2 + s_j^2 = 1$, Equation (2) is transferred to a system of polynomial equations:

$$\begin{aligned}
 f_1 &= 112c_1c_4s_7 - 16c_1c_4 + 112c_1s_4c_7 + 136c_1s_4 - 44\sqrt{2}c_1 + x = 0, \\
 f_2 &= 112s_1c_4s_7 - 16s_1c_4 + 112s_1s_4c_7 + 136s_1s_4 - 44\sqrt{2}s_1 + y = 0, \\
 f_3 &= -112c_4c_7 - 136c_4 + 112s_4s_7 - 16s_4 - 104 - 44\sqrt{2} + z = 0, \\
 f_4 &= s_1^2 + c_1^2 - 1 = 0, \quad f_5 = s_4^2 + c_4^2 - 1 = 0, \quad f_6 = s_7^2 + c_7^2 - 1 = 0. \tag{3}
 \end{aligned}$$

3. Real quantifier elimination based on CGS

Equation (3) shows that solving the inverse kinematic problem for the given system can be regarded as a real quantifier elimination of a quantified formula

$$\exists c_1 \exists s_1 \exists c_4 \exists s_4 \exists c_7 \exists s_7 \\ (f_1 = 0 \wedge f_2 = 0 \wedge f_3 = 0 \wedge f_4 = 0 \wedge f_5 = 0 \wedge f_6 = 0), \quad (4)$$

with x, y, z as parameters.

In this section, we briefly review an algorithm of real quantifier elimination based on CGS, the CGS-QE algorithm, by Fukasaku et al. [7]. Two main tools play a crucial role in the algorithm: one is CGS, and another is real root counting, or counting the number of real roots of a system of polynomial equations. Note that, in this paper, we only consider equations in the quantified formula.

Hereafter, let R be a real closed field, C be the algebraic closure of R , and K be a computable subfield of R . In this paper, we consider R as the field of real numbers \mathbb{R} , C as the field of complex numbers \mathbb{C} , and K as the field of rational numbers \mathbb{Q} . Let \bar{X} and \bar{A} denote variables X_1, \dots, X_n and A_1, \dots, A_m , respectively, and $T(\bar{X})$ be the set of the monomials which consist of variables in \bar{X} . For an ideal $I \subset K[\bar{X}]$, let $V_R(I)$ and $V_C(I)$ be the affine varieties of I in R or C , respectively, satisfying that $V_R(I) = \{\bar{c} \in R^n \mid \forall f(\bar{X}) \in I: f(\bar{c}) = 0\}$ and $V_C(I) = \{\bar{c} \in C^n \mid \forall f(\bar{X}) \in I: f(\bar{c}) = 0\}$.

3.1. CGS

For the detail and algorithms on CGS, see Fukasaku et al. [7] or references therein. In this paper, the following notation is used. Let \succ be an admissible term order. For a polynomial $f \in K[\bar{A}, \bar{X}]$ with a term order \succ on $T(\bar{X})$, we regard f as a polynomial in $(K[\bar{A}])[\bar{X}]$, which is the ring of polynomials with \bar{X} as variables and coefficients in $(K[\bar{A}])$ such that \bar{A} is regarded as parameters. Given a term order \succ on $T(\bar{X})$, $\text{LT}(f)$, $\text{LC}(f)$ and $\text{LM}(f)$ denotes the leading term, the leading coefficient, and the leading monomial, respectively, satisfying that $\text{LT}(f) = \text{LC}(f)\text{LM}(f)$ with $\text{LC}(f) \in K[\bar{A}]$ and $\text{LM} \in T(\bar{X})$ (we follow the notation by Cox et al. [4]).

Definition 1 (Algebraic partition and Segment). Let $S \subset C^m$ for $m \in \mathbb{N}$. A finite set $\{\mathcal{S}_1, \dots, \mathcal{S}_t\}$ of nonempty subsets of S is called an algebraic partition of S if it satisfies the following properties:

1. $S = \bigcup_{k=1}^t \mathcal{S}_k$.
2. For $k \neq j \in \{1, \dots, t\}$, $\mathcal{S}_k \cap \mathcal{S}_j = \emptyset$.
3. For $k \in \{1, \dots, t\}$, \mathcal{S}_k is expressed as $\mathcal{S}_k = V_C(I_1) \setminus V_C(I_2)$ for some ideals $I_1, I_2 \subset K[\bar{A}]$.

Furthermore, each \mathcal{S}_k is called a segment.

Definition 2 (Comprehensive Gröbner System (CGS)). Let $S \subset C^m$ and \succ be a term order on $T(\bar{X})$. For a finite subset $F \subset K[\bar{A}, \bar{X}]$, a finite set $\mathcal{G} = \{(\mathcal{S}_1, G_1), \dots, (\mathcal{S}_t, G_t)\}$ is called a Comprehensive Gröbner System

(CGS) of F over \mathcal{S} with parameters \bar{A} with respect to \succ if it satisfies the following:

1. For $k \in \{1, \dots, t\}$, G_k is a finite subset of $K[\bar{A}, \bar{X}]$.
2. The set $\{\mathcal{S}_1, \dots, \mathcal{S}_t\}$ is an algebraic partition of \mathcal{S} .
3. For each $\bar{c} \in \mathcal{S}_k$, $G_k(\bar{c}, \bar{X}) = \{g(\bar{c}, \bar{X}) \mid g(\bar{A}, \bar{X}) \in G_k\}$ is a Gröbner basis of the ideal $\langle F(\bar{c}, \bar{X}) \rangle \subset C[\bar{X}]$ with respect to \succ , where $F(\bar{c}, \bar{X}) = \{f(\bar{c}, \bar{X}) \mid f(\bar{A}, \bar{X}) \in F\}$.
4. For each $\bar{c} \in \mathcal{S}_k$, any $g \in G_k$ satisfies that $(LC(g))(\bar{c}) \neq 0$.

Furthermore, if each $G_k(\bar{c}, \bar{X})$ is a minimal or the reduced Gröbner basis, \mathcal{G} is called a minimal or the reduced CGS, respectively. In the case $\mathcal{S} = C^m$, the words “over \mathcal{S} ” may be omitted.

3.2. Real root counting

Let $I \subset K[\bar{X}]$ be a zero dimensional ideal. Then, the quotient ring $K[\bar{X}]/I$ is regarded as a finite dimensional vector space over K [3]; let $\{v_1, \dots, v_d\}$ be its basis. For $h \in K[\bar{X}]/I$ and i, j satisfying $1 \leq i, j \leq d$, let $\theta_{h,i,j}$ be a linear transformation defined as

$$\begin{array}{ccc} \theta_{h,i,j} : K[\bar{X}]/I & \longrightarrow & K[\bar{X}]/I \\ \cup & & \cup \\ f & \mapsto & hv_i v_j f \end{array} .$$

Let $q_{h,i,j}$ be the trace of $\theta_{h,i,j}$ and M_h^I be a symmetric matrix such that its (i, j) -th element is given by $q_{h,i,j}$. Let $\chi_h^I(X)$ be the characteristic polynomial of M_h^I , and $\sigma(M_h^I)$, called the signature of M_h^I , be the number of positive eigenvalues of M_h^I minus the number of negative eigenvalues of M_h^I . Then, we have the following theorem on the real root counting [1, 21].

Theorem 3 (The real root counting theorem). *We have*

$$\sigma(M_h^I) = \#\{\bar{c} \in V_R(I) \mid h(\bar{c}) > 0\} - \#\{\bar{c} \in V_R(I) \mid h(\bar{c}) < 0\}.$$

Corollary 4. $\sigma(M_1^I) = \#(V_R(I))$.

Since we only consider a quantified formula with equations, as in Equation (4), we omit properties of the real root counting related to quantifier elimination of quantified formula with inequalities or inequations (for detail, see Fukasaku et al. [7]).

3.3. CGS-QE algorithm

The CGS-QE algorithm accepts the following quantified formula given as

$$\begin{aligned} \exists \bar{X} (f_1(\bar{A}, \bar{X}) = 0 \quad \wedge \quad \cdots \quad \wedge \quad f_\rho(\bar{A}, \bar{X}) = 0 \quad \wedge \\ p_1(\bar{A}, \bar{X}) > 0 \quad \wedge \quad \cdots \quad \wedge \quad p_\sigma(\bar{A}, \bar{X}) > 0 \quad \wedge \\ q_1(\bar{A}, \bar{X}) \neq 0 \quad \wedge \quad \cdots \quad \wedge \quad q_\tau(\bar{A}, \bar{X}) \neq 0), \\ f_1, \dots, f_\rho, p_1, \dots, p_\sigma, q_1, \dots, q_\tau \in \mathbb{Q}[\bar{A}, \bar{X}] \setminus \mathbb{Q}[\bar{A}], \end{aligned}$$

then outputs an equivalent quantifier-free formula. Note that, in this paper, we give a quantified formula only with equations as shown in Equation (4). The algorithm is divided into several algorithms. The main algorithm is called **MainQE** and sub-algorithms are called **ZeroDimQE** and

NonZeroDimQE for the case that the ideal generated by the component of the CGS is zero-dimensional or positive dimensional, respectively. (For a complete description of the algorithm, see Fukasaku et al. [7].)

In the real root counting, we need to calculate $\sigma(M_h^I)$ as in Section 3.2. This calculation is executed using the following property [32] derived from Descartes' rule of signs. Let M be a real symmetric matrix of dimension d and $\chi(X)$ be the characteristic polynomial of M of degree d , expressed as

$$\begin{aligned}\chi(\lambda) &= \lambda^d + a_{d-1}\lambda^{d-1} + \dots + a_0, \\ \chi(-\lambda) &= (-1)^d\lambda^d + b_{d-1}\lambda^{d-1} + \dots + b_0.\end{aligned}$$

Note that $b_\ell = a_\ell$ if ℓ is even, and $b_\ell = -a_\ell$ if ℓ is odd. Let $L_{\chi+}$ and $L_{\chi-}$ be the sequence of the coefficients in $\chi(\lambda)$ and $\chi(-\lambda)$, defined as

$$L_{\chi+} = (1, a_{d-1}, \dots, a_0), \quad L_{\chi-} = ((-1)^d, b_{d-1}, \dots, b_0), \quad (5)$$

respectively. Furthermore, let $\bar{L}_{\chi+}$ and $\bar{L}_{\chi-}$ be the sequences defined by removing zero coefficients in $L_{\chi+}$ and $L_{\chi-}$, respectively, and let

$$\begin{aligned}S_{\chi+} &= (\text{the number of sign changes in } \bar{L}_{\chi+}), \\ S_{\chi-} &= (\text{the number of sign changes in } \bar{L}_{\chi-}).\end{aligned} \quad (6)$$

Then, we have the following.

Lemma 5. *Let $S_{\chi+}$ and $S_{\chi-}$ be defined as in Equation (6). Then, we have*

$$S_{\chi+} = \#\{c \in \mathbb{R} \mid c > 0 \wedge \chi(c) = 0\}, \quad S_{\chi-} = \#\{c \in \mathbb{R} \mid c < 0 \wedge \chi(c) = 0\}.$$

Corollary 6. *Let $S_{\chi+}$ and $S_{\chi-}$ be defined as in Equation (6), and I be a zero dimensional ideal and M_1^I be a matrix as in Section 3.2. Then, we have*

$$\#(V_R(I)) = \sigma(M_1^I) = S_{\chi+} - S_{\chi-}. \quad (7)$$

3.4. Applying the CGS-QE algorithm for verification of real roots in the inverse kinematics problem

We note that while the CGS-QE algorithm outputs an unquantified formula for the given quantified formula, we apply the CGS-QE algorithm for verifying (or counting the actual number of) real roots in the inverse kinematic problem, which means that we may not necessarily derive an unquantified formula in the inverse kinematic computation.

In the CGS-QE algorithm [7], for the quantified formula (4), Equation (7) shows that

$$\#(V_R(I)) = \sigma(M_1^I) > 0 \Leftrightarrow S_{\chi+} \neq S_{\chi-}.$$

In Equation (5), by regarding a_{d-1}, \dots, a_0 as variables, $S_{\chi+} \neq S_{\chi-}$ can be expressed as a quantifier free first order formula, denoted as $I_d(a_0, \dots, a_{d-1})$. Then, Equation (4) is expressed as an unquantified formula as

$$(f_1 = 0 \wedge f_2 = 0 \wedge f_3 = 0 \wedge f_4 = 0 \wedge f_5 = 0 \wedge f_6 = 0) \wedge I_d(a_0, \dots, a_{d-1}).$$

On the other hand, in verifying the existence of real roots in the inverse kinematic problem, the coefficients of the characteristic polynomial $\chi(X)$ contain x, y, z , so do the elements in $L_{\chi+}$ and $L_{\chi-}$. Then, by substituting

x, y, z with the given coordinates of the end-effector, respectively, the values S_{χ^+} and S_{χ^-} in Equation (6) are decided. Finally, with Equation (7), we calculate the number of real roots for verifying the existence of real roots of the inverse kinematic problem.

4. Solving the inverse kinematic problem with the CGS-QE algorithm

Let us consider the following inverse kinematic problem: the manipulator consists of Joint $0, \dots, t+1$ with the coordinate system $\Sigma_0, \dots, \Sigma_{t+1}$, respectively, where Joint 0 represents the perpendicular foot on the ground from Joint 1 and Joint $t+1$ represents the end-effector as the example above. For $j = 1, \dots, t$, let θ_j be the angle between axes x_{j-1} and x_j with respect to the z_j axis. Let (x, y, z) be the position of end-effector with respect to Σ_0 , expressed as

$$f_1(\bar{A}, \bar{X}) = 0, \dots, f_w(\bar{A}, \bar{X}) = 0, \quad (8)$$

with $f_i(\bar{A}, \bar{X}) \in \mathbb{Q}[\bar{A}, \bar{X}]$, $\bar{A} = (x, y, z)$, $\bar{X} = (X_1, \dots, X_{2t})$, $X_{2j-1} = \cos \theta_j$, $X_{2j} = \sin \theta_j$ for $j = 1, \dots, t$.

Let $\bar{c} = (\alpha, \beta, \gamma) \in \mathbb{R}^3$ be a position of the end-effector. For solving the inverse kinematic problem, we first verify the existence of real roots in the polynomial equations

$$f_1(\bar{c}, \bar{X}) = 0, \dots, f_w(\bar{c}, \bar{X}) = 0, \quad (9)$$

using the CGS-QE algorithm. If Equation (9) has real roots, solve the system of equation numerically: let $(X_1, \dots, X_{2t}) = (\psi_1, \varphi_1, \psi_2, \varphi_2, \dots, \psi_t, \varphi_t)$ be a solution. Then, a configuration of the joints is calculated as

$$\theta_1 = \arctan(\varphi_1/\psi_1), \theta_2 = \arctan(\varphi_2/\psi_2), \dots, \theta_t = \arctan(\varphi_t/\psi_t). \quad (10)$$

Our method of solving the inverse kinematic problem consists of *preprocessing* steps as shown in Algorithm 1, followed by *main* steps as shown in Algorithm 2. Note that Algorithm 1 (the preprocessing steps) is executed for once prior to solving the inverse kinematic problem, then Algorithm 2 (the main steps) is executed every time for solving the inverse kinematic problem.

In Algorithm 1, the output \mathcal{G} satisfies that each segment S_k in \mathcal{G} contains real points and the system of polynomial equations (9) has finite number of roots for $\bar{c} \in S_k$. (Note that, at this point, the roots may not be real numbers.) Furthermore, Algorithm 1 follows the CGS-QE algorithm (for zero-dimensional case) in Fukasaku et al. [7] as follows.

- Line 2 corresponds to line 2 in Algorithm 1 (MainQE).
- In line 4, the condition $G_k(\bar{c}, \bar{X}) \neq \{0\}$ corresponds to line 6 in Algorithm 1 (MainQE), and the condition $\langle G_k(\bar{c}, \bar{X}) \rangle \neq \langle 1 \rangle$ corresponds to line 1 in Algorithm 2 (ZeroDimQE).
- Line 5 corresponds to line 9 in Algorithm 1 (MainQE).

Algorithm 1 Preprocessing steps

Input: $f_1, \dots, f_w \in \mathbb{Q}[\bar{A}, \bar{X}]$ in Equation (9), \succ : a term order on $T(\bar{X})$;

Output: $\mathcal{G} = \{(\mathcal{S}_1, G_1, \chi_1(\lambda)), \dots, (\mathcal{S}_\mu, G_\mu, \chi_\mu(\lambda))\}$

```

1:  $\mathcal{G} \leftarrow \emptyset$ ;
2:  $\mathcal{F} = \{(\mathcal{S}_1, G_1), \dots, (\mathcal{S}_\mu, G_\mu)\} \leftarrow$  (a CGS of  $\langle f_1, \dots, f_w \rangle$  with respect to  $\succ$ );
3: for  $k = 1, \dots, \mu$  do
4:   if  $\mathcal{S}_k \cap \mathbb{R}^3 \neq \emptyset \wedge \forall \bar{c} \in \mathcal{S}_k (G_k(\bar{c}, \bar{X}) \neq \{0\} \wedge (\langle G_k(\bar{c}, \bar{X}) \rangle \neq \langle 1 \rangle))$ 
     then
5:     if  $(\forall \bar{c} \in \mathcal{S}_k (\langle G_k(\bar{c}, \bar{X}) \rangle$  is zero-dimensional)) then
6:        $M_1^{I_k} \leftarrow$  (the matrix defined as in Section 3.2 with  $I_k = \langle G_k(\bar{c}, \bar{X}) \rangle$ );
7:        $\chi_k(\lambda) \leftarrow$  (the characteristic polynomial of  $M_1^{I_k}$ );
8:        $\mathcal{G} \leftarrow \mathcal{G} \cup \{(\mathcal{S}_k, G_k, \chi_k(\lambda))\}$ ;
9:     else
10:      Let  $\bar{A}' \subset \bar{A}$  and  $\bar{X}' \subset \bar{X}$ ;
11:      For  $G_k = (g_{k,1}(\bar{A}, \bar{X}), \dots, g_{k,u_k}(\bar{A}, \bar{X}))$ , define
            $h_{k,1}(\bar{A}', \bar{X}'), \dots, h_{k,u'}(\bar{A}', \bar{X}') \subset \mathbb{Q}[\bar{A}', \bar{X}']$ 
           by setting appropriate constants to  $\bar{A} \setminus \bar{A}'$  and  $\bar{X} \setminus \bar{X}'$ 
           in  $g_{k,1}(\bar{A}, \bar{X}), \dots, g_{k,u_k}(\bar{A}, \bar{X})$ ;
12:       $\mathcal{G} \leftarrow \mathcal{G} \cup$ (Output of Algorithm 1 with  $h_{k,1}(\bar{A}', \bar{X}'), \dots, h_{k,u'}(\bar{A}', \bar{X}')$ );
13:     end if
14:   end if
15: end for
16: return  $\mathcal{G}$ ;
```

- Lines 6 and 7 correspond to lines 5, 6, and 7 in Algorithm 2 (ZeroDimQE), and the result is used in verifying the existence of real roots for the given coordinates of the end-effector in Algorithm 2.

In line 5 of Algorithm 1, in the case the ideal $\langle G_k(\bar{c}, \bar{X}) \rangle$ is not zero-dimensional, the system of polynomial equations $\{g(\bar{c}, \bar{X}) = 0 \mid g \in G_k(\bar{c}, \bar{X})\}$ satisfies that, for some variables, say $\bar{X}' \subset \bar{X}$, the solution is not unique. In this case, we set a solution to \bar{X}' , and, if necessary, choose a subset of parameters $\bar{A}' \subset \bar{A}$, then define polynomials $h_{k,j}(\bar{A}', \bar{X}')$, and call Algorithm 1 recursively. This computation is described as in lines 10–12, and our example is described in Section 4.2.

In Algorithm 2, for the given position of the end-effector $\bar{c} = (\alpha, \beta, \gamma)$, we verify if there exist real roots of Equation (9): if there do, then, solve Equation (9) and calculate the configuration of the joints.

In the following, we explain our implementation³ [26] and observations in computation details of the proposed algorithms for our example above.

³In the following footnotes, file locations are described as the relative path from the top directory of the software repository [26].

⁴Note that, in the programs and the log files of Risa/Asir, index runs from 0 to $n - 1$, while, in the results in the present paper and the notebook files of Mathematica, it runs from 1 to n .

Algorithm 2 Main steps

Input: $\mathcal{G} = \{(\mathcal{S}_1, G_1, \chi_1(\lambda)), \dots, (\mathcal{S}_u, G_u, \chi_u(\lambda))\}$: the output of Algorithm 1, with $G_k = (g_{k,1}(\bar{A}, \bar{X}), \dots, g_{k,u_k}(\bar{A}, \bar{X}))$; $\bar{c} = (\alpha, \beta, \gamma) \in \mathbb{R}^3$: a position of the end-effector;

Output: $(\theta_1, \dots, \theta_t)$: a solution of Equation (9) (if exists for $\bar{c} = (\alpha, \beta, \gamma)$);

```

1: Find  $k \in \{1, \dots, u\}$  satisfying that  $\bar{c} \in \mathcal{S}_k$ ;
2: if  $\nexists k \in \{1, \dots, u\}$  satisfying that  $\bar{c} \in \mathcal{S}_k$  then
3:   return  $\emptyset$ ;
4: else
5:    $\bar{\chi}_k(\lambda) \leftarrow$  (set  $x \leftarrow \alpha, y \leftarrow \beta, z \leftarrow \gamma$  in  $\chi_k(\lambda)$ );
6:   Calculate  $S_{\bar{\chi}_k+}, S_{\bar{\chi}_k-}$  as in Equation (6);
7:   if  $S_{\bar{\chi}_k+} - S_{\bar{\chi}_k-} = 0$  then ▷ Corollary 6
8:     return  $\emptyset$ ;
9:   else ▷ There exists real roots of Equation (9)
10:     $(\varphi_1, \psi_1, \dots, \varphi_t, \psi_t) \leftarrow$  (a solution of  $g_{k,1}(\bar{c}, \bar{X}) = \dots = g_{k,u_k}(\bar{c}, \bar{X}) = 0$ );
11:    for  $j = 1, \dots, t$  do
12:       $\theta_j \leftarrow \arctan(\varphi_j/\psi_j)$ ;
13:    end for
14:    return  $(\theta_1, \dots, \theta_t)$ ;
15:  end if
16: end if
    
```

4.1. Algorithm 1

In Algorithm 1, computation of CGS was executed with the computer algebra system Risa/Asir and the rest of computation was executed by hand with Risa/Asir and Wolfram Mathematica 12.0.0.

4.1.1. Computation of CGS. For $f_1, \dots, f_6 \in \mathbb{Q}[\bar{A}, \bar{X}]$ in Equation (4), a CGS of the ideal $\langle f_1, \dots, f_6 \rangle$ has been computed with respect to lexicographic order (“lexicographic” is abbreviated as the “lex” order) with

$$c_1 \succ s_1 \succ c_4 \succ s_4 \succ c_7 \succ s_7^5. \quad (11)$$

Computation of CGS was executed with the implementation of CGS computation by Nabeshima [16] on Risa/Asir. We have obtained a CGS with the algebraic partition consisting of 33 segments in approximately 66.7 seconds using the computing environment as shown in Section 6. Let \mathcal{F} be the computed CGS, expressed as

$$\mathcal{F} = \{(\mathcal{S}_1, G_1), \dots, (\mathcal{S}_{33}, G_{33})\}^6,$$

⁵Since Equation (4) is fully existentially quantified formula and an order on the variables do not affect the output, any order on the variables can be used. For future research direction, see Section 7.

⁶The output code is available in Risa/Asir format as `preprocessing-steps/cgs/F.rr` (text file, approximately 800 KB) and `preprocessing-steps/cgs/F.dat` (binary file, approximately 1 MB). Each G_k is recorded as in `preprocessing-steps/cgs/F-basis/G-(k-1).rr`.

with $\mathcal{S}_k = V_{\mathbb{C}}(I_{k,1}) \setminus V_{\mathbb{C}}(I_{k,2})$, $I_{k,1} = \langle F_{k,1} \rangle$, $I_{k,2} = \langle F_{k,2} \rangle^7$ satisfying that $F_{k,1}, F_{k,2} \subset \mathbb{Q}[x, y, z]$.

4.1.2. Verifying $\mathcal{S}_k \cap \mathbb{R}^3 \neq \emptyset$. We have verified the segments that contain real points as follows.

1. There exists a point in $V_{\mathbb{R}}(I_{k,1})$, explicitly found, which does not belong to $V_{\mathbb{R}}(I_{k,2})$ (for $k = 1, 2, 3$).
2. With the discriminant or the QE computation, we see that there exists a point in $V_{\mathbb{R}}(I_{k,1})$. Let $G_{k,1}$ be a Gröbner basis of $I_{k,1}$ with respect to lex order with $x \succ y \succ z$, and, for $f \in F_{k,2}$, the remainder of f divided by $G_{k,1}$ is not equal to zero (for $k = 6, 9, 11, 13, 15, 18, 19, 25, 31, 32$). The discriminant, the Gröbner basis and the QE computation were executed with Mathematica.
3. There exists a point in $V_{\mathbb{R}}(I_{k,1})$ and $V_{\mathbb{C}}(I_{k,2}) = \emptyset$ (for $k = 30$).
4. We have $V_{\mathbb{C}}(I_{k,1}) = \mathbb{C}^3$ and the QE computation shows that there exists a real point which is not contained in $V_{\mathbb{C}}(I_{k,2})$ (for $k = 33$). The QE computation was executed with Mathematica.

Summarizing above⁸, we have $\mathcal{S}_k \cap \mathbb{R}^3 \neq \emptyset$ for

$$k \in \{1, 2, 3, 6, 9, 11, 13, 15, 18, 19, 25, 30, 31, 32, 33\}. \quad (12)$$

4.1.3. Verifying $G_k(\bar{c}, \bar{X}) \neq \{0\}$ for $\bar{c} \in \mathcal{S}_k$. For k in Equation (12), by Property 4 of Definition 2, G_k satisfies that $G_k(\bar{c}, \bar{X}) \neq \{0\}$ for $\bar{c} \in \mathcal{S}_k$.

4.1.4. Verifying $\langle G_k(\bar{c}, \bar{X}) \rangle \neq \langle 1 \rangle$ for $\bar{c} \in \mathcal{S}_k$. For k in Equation (12) satisfying $k \notin \{3, 30\}$, by Property 4 of Definition 2, G_k satisfies that $\langle G_k(\bar{c}, \bar{X}) \rangle \neq \langle 1 \rangle$ for $\bar{c} \in \mathcal{S}_k$.

4.1.5. Verifying $\langle G_k(\bar{c}, \bar{X}) \rangle$ is zero-dimensional for $\bar{c} \in \mathcal{S}_k$. According to the ‘‘Finiteness Theorem’’ [4, Chapter 5, Section 3, Theorem 6], for k in Equation (12) satisfying $k \notin \{3, 30\}$, G_k satisfies that $\langle G_k(\bar{c}, \bar{X}) \rangle$ is zero-dimensional for $\bar{c} \in \mathcal{S}_k$ ⁹. For $k \in \{3, 30\}$, (F_k, G_k) will be processed with Algorithm 1 that is called recursively (see Section 4.2).

4.1.6. Computation of $M_1^{F_k}$ and $\chi_k(\lambda)$. For k in Equation (12) satisfying $k \notin \{3, 30\}$, the matrix $M_1^{F_k}$ and its characteristic polynomial $\chi_k(\lambda)$ have been calculated with our implementation on Risa/Asir. Then, simplification of polynomial expressions on $\chi_k(\lambda)$ has been executed with Mathematica. For example, the output of Risa/Asir has a power of $2^{(1/2)}$ such as $(2^{(1/2)})^4$ as in the form of $(2 \wedge (1/2)) \wedge 4$, thus, with Mathematica, we apply `Simplify` function to simplify $(2^{(1/2)})^4$ to 4.

⁷For \mathcal{S}_k , $F_{k,1}$ and $F_{k,2}$ are recorded in the directory `preprocessing-steps/cgs/F-segments` as `F-(k-1)-1.rr` and `F-(k-1)-2.rr`, respectively.

⁸The computation was summarized as a Mathematica notebook file `preprocessing-steps/cgs/F-segments/F-verification.nb`.

⁹The computation was executed with Risa/Asir with the program file `preprocessing-steps/cgs/zero-dimensional-test.rr` and the log file `preprocessing-steps/cgs/zero-dimensional-test.log`.

4.2. A recursive call of Algorithm 1

For $k \in \{3, 30\}$, we see that $\langle G_k(\bar{c}, \bar{X}) \rangle$ is not zero-dimensional because there does not exist $g \in G_k$ satisfying that $\text{LM}(g) = s_1^{m_1}$ with $m_1 > 0$. Note that, for $k \in \{3, 30\}$, $c_1^2 + s_1^2 - 1 \in G_k$. On the other hand, for $k \in \{3, 30\}$, the points in $V_{\mathbb{R}}(I_{k,1})$ satisfy $x = y = 0$. This means that the end-effector is located on the z -axis and θ_1 , the angle of Joint J_1 , is not uniquely determined. Thus, by setting $x = y = 0$ and $\theta_1 = 0$ (i.e. $c_1 = 1, s_1 = 0$) in Equation (3), we have the following system of equations.

$$\begin{aligned} h_1 &= 112c_4s_7 - 16c_4 - 112s_4c_7 + 136s_4 - 44\sqrt{2} = 0, \\ h_2 &= 112c_4c_7 + 136c_4 - 112s_4s_7 + 16s_4 + 44\sqrt{2} + 104 - z = 0, \\ h_3 &= s_4^2 + c_4^2 - 1 = 0, \quad h_4 = s_7^2 + c_7^2 - 1 = 0. \end{aligned} \quad (13)$$

Note that, in Equation (13), f_2 in Equation (3) vanishes by putting $s_1 = 0$, f_4 is eliminated, and f_1, f_3, f_5, f_6 are replaced with h_1, h_2, h_3, h_4 , respectively.

We have recursively applied Algorithm 1 to $\{h_1, h_2, h_3, h_4\}$ in Equation (13), as follows. The implementation used in each step is the same as the one used in the corresponding step in the original call of Algorithm 1 as in above.

4.2.1. Computation of CGS. We have obtained a CGS with the algebraic partition consisting of 3 segments in approximately 0.0142 seconds using the computing environment as shown in Section 6. Let \mathcal{H} be the computed CGS, expressed as

$$\mathcal{H} = \{(\mathcal{S}_{34}, G_{34}), (\mathcal{S}_{35}, G_{35}), (\mathcal{S}_{36}, G_{36})\}^{10},$$

with $\mathcal{S}_k = V_{\mathbb{C}}(I_{k,1}) \setminus V_{\mathbb{C}}(I_{k,2})$, $I_{k,1} = \langle F_{k,1} \rangle$, $I_{k,2} = \langle F_{k,2} \rangle^{11}$ ($k = 34, 35, 36$) satisfying that $F_{k,1}, F_{k,2} \subset \mathbb{Q}[z]$.

4.2.2. Verifying conditions for \mathcal{S}_k . We have $\mathcal{S}_k \cap \mathbb{R}^3 \neq \emptyset$ only for $k = 36$, with $V_{\mathbb{C}}(I_{36,1}) = \mathbb{C}$ and the discriminant computation shows that none of the real point is contained in $V_{\mathbb{C}}(I_{36,2})^{12}$. Furthermore, for $\bar{c} \in \mathcal{S}_{36}$, $(\mathcal{S}_{36}, G_{36})$ satisfies that $G_{36}(\bar{c}, \bar{X}) \neq \{0\}$, $\langle G_{36}(\bar{c}, \bar{X}) \rangle \neq \langle 1 \rangle$ and $\langle G_{36}(\bar{c}, \bar{X}) \rangle$ is zero-dimensional¹³.

4.2.3. Computation of $M_1^{I_k}$ and $\chi_k(\lambda)$. For $(\mathcal{S}_{36}, G_{36})$, The matrix $M_1^{I_{36}}$ and its characteristic polynomial $\chi_{36}(\lambda)$ have been calculated, and $\mathcal{G} = \{(\mathcal{S}_{36}, G_{36}, \chi_{36}(\lambda))\}$ has been returned to the original call of Algorithm 1.

¹⁰The output code is available in Risa/Asir format as `preprocessing-steps/cgs/H.rr` (text file, approximately 1.8 KB) and `preprocessing-steps/cgs/H.dat` (binary file, approximately 7 KB). Each G_k is recorded as in `preprocessing-steps/cgs/H-basis/G-(k-1).rr`.

¹¹For \mathcal{S}_k , $F_{k,1}$ and $F_{k,2}$ are recorded in the directory `preprocessing-steps/cgs/H-segments` as `F-(k-1)-1.rr` and `F-(k-1)-2.rr`, respectively.

¹²The computation was summarized as a Mathematica notebook file `preprocessing-steps/cgs/H-segments/H-verification.nb`.

¹³The verification of zero-dimensional is recorded in the same file as in Footnote 9.

4.3. Algorithm 1 (continued)

Now we return to the original call of Algorithm 1 as in Section 4.1. As a consequence, Algorithm 1 has returned the following output:

$$\begin{aligned} \mathcal{G} &= \{(S_k, G_k, \chi_k(\lambda)) \mid k \in I'\}, \\ I' &= \{1, 2, 6, 9, 11, 13, 15, 18, 19, 25, 31, 32, 33, 36\}. \end{aligned} \tag{14}$$

4.4. Algorithm 2

Algorithm 2 is implemented using SymPy on the top of Python and Risa/Asir connected with OpenXM infrastructure for communicating mathematical software systems, as the implementation in our previous research [8]. A difference between our previous and present implementations is the purpose of the use of Risa/Asir. While Risa/Asir has been used for computing Gröbner bases in our previous implementation, now it is used for the real root counting in the present implementation.

4.4.1. Substituting x, y, z in $\chi_k(\lambda)$ with $\bar{c} = (\alpha, \beta, \gamma)$. For substituting x, y, z in $\chi_k(\lambda)$, we first tried using Python for the entire step. However, a preliminary experiment had shown that it took approximately 2 seconds for substituting x, y, z in the coefficients for some characteristic polynomials with the given position of the end-effector $\bar{c} = (\alpha, \beta, \gamma)$ with SymPy, although it took approximately 0.01 seconds to count the number of sign changes of the sequence of coefficients, which was sufficiently fast. Thus, we decided to use Risa/Asir for substituting x, y, z with $\bar{c} = (\alpha, \beta, \gamma)$, which is executed in approximately 0.2 seconds, and continue to use Python for counting the number of sign changes of the sequence of coefficients.

4.4.2. Solving the system of polynomial equations. First, we remark on the form of the Gröbner bases computed and re-organization of some of them. For $k \in I' \setminus \{18, 25, 31, 32\}$, where I' is as shown in Equation (14), we see that the Gröbner basis $G_k = \{g_{k,1}, \dots, g_{k,6}\}$ has a shape form such that

$$\begin{aligned} g_{k,1} &= g_{k,1}(s_7), & \text{LM}(g_{k,2}) &= c_7, \\ g_{k,2} &= g_{k,2}(c_7, s_7), & \text{LM}(g_{k,3}) &= s_4, \\ g_{k,3} &= g_{k,3}(s_4, c_7, s_7), & \text{LM}(g_{k,4}) &= c_4, \\ g_{k,4} &= g_{k,4}(c_4, s_4, c_7, s_7), & \text{LM}(g_{k,5}) &= s_1, \\ g_{k,5} &= g_{k,5}(s_1, c_7, s_7), & \text{LM}(g_{k,6}) &= c_1. \\ g_{k,6} &= g_{k,6}(c_1, s_1, c_7, s_7), \end{aligned}$$

On the other hand, for $k \in \{18, 25, 31, 32\}$, $G_k = \{g_{k,1}, \dots, g_{k,7}\}$ with

$$\begin{aligned} g_{k,1} &= g_{k,1}(s_7), \\ g_{k,2} &= g_{k,2}(c_7, s_7), & \text{LM}(g_{k,2}) &= c_7 s_7, \\ g_{k,3} &= c_7^2 + s_7^2 - 1, \\ g_{k,4} &= g_{k,4}(s_4, c_7, s_7), & \text{LM}(g_{k,4}) &= s_4, \\ g_{k,5} &= g_{k,5}(c_4, s_4, c_7, s_7), & \text{LM}(g_{k,5}) &= c_4, \\ g_{k,6} &= g_{k,6}(s_1, c_7, s_7), & \text{LM}(g_{k,6}) &= s_1, \\ g_{k,7} &= g_{k,7}(c_1, s_1, c_7, s_7), & \text{LM}(g_{k,7}) &= c_1. \end{aligned}$$

In the above formula, $g_{k,2}(c_7, s_7)$ has a term of s_7^2 . Thus, let $g'_{k,2}(c_7, s_7)$ be the result of substituting the term of s_7^2 in $g_{k,2}(c_7, s_7)$ with $1 - c_7^2$, then we have $\text{LM}(g'_{k,2}) = c_7^2$. Furthermore, let $G'_i = \{g_{k,1}, g'_{k,2}, g_{k,4}, \dots, g_{k,7}\}$. For example, in the case $i = 18$, we have

$$\begin{aligned} g_{18,2} &= -1113167888c_7s_7 - 1046586912c_7 + 4665483060s_7^2 \\ &\quad + 123127872s_7 + 4239831888. \end{aligned}$$

By substituting s_7^2 with $1 - c_7^2$, we have

$$\begin{aligned} g'_{18,2} &= 4665483060c_7^2 - 1113167888c_7s_7 - 1046586912c_7 \\ &\quad + 123127872s_7 - 425651172, \end{aligned}$$

with $\text{LM}(g'_{18,2}) = c_7^2$ ¹⁴.

As a result, for solving the system of polynomial equations, G_k for $k \in I' \setminus \{18, 25, 31, 32\}$ and G'_k for $k \in \{18, 25, 31, 32\}$ are used¹⁵.

The form of the Gröbner bases above shows that the system of polynomial equations can be solved by solving univariate equations successively, as follows. For $k \in I' \setminus \{18, 25, 31, 32\}$, solve $g_{k,1}(s_7) = 0$ and let φ_7 be the calculated root. Next, solve $g_{k,2}(c_7, \varphi_7) = 0$ for c_7 after substituting s_7 with φ_7 , and let ψ_7 be the calculated root. Then, solve $g_{k,3}(s_4, \psi_7, \varphi_7) = 0$ for s_4 and $g_{k,5}(s_1, \psi_7, \varphi_7) = 0$ for s_1 after substituting c_7 and s_7 with ψ_7 and φ_7 , respectively, and let φ_4 and φ_1 be the calculated roots, respectively. Finally, solve $g_{k,5}(c_4, \varphi_1, \psi_7, \varphi_7) = 0$ for c_4 and $g_{k,6}(c_1, \varphi_1, \psi_7, \varphi_7) = 0$ for c_1 after substituting s_1, s_4, c_7, s_7 with $\varphi_1, \varphi_4, \psi_7, \varphi_7$, respectively, and let ψ_4 and ψ_1 be the calculated roots, respectively. For $k \in \{18, 25, 31, 32\}$, the system of polynomial equations can be solved similarly.

For solving the system of polynomial equations with Python, we use a numerical solver in Python's NumPy package [29] (`numpy.roots`) solving univariate equations, according to our observation in our previous research

¹⁴For $k = 18, 25, 31, 32$, computation of $g'_{k,2}$ is saved in a Mathematica notebook file `main-steps/present-method/substitute-s7squared.nb`.

¹⁵The check of shape form was executed with Risa/Asir with the program file `main-steps/present-method/shape-form-test.rr` and the log file `main-steps/present-method/shape-form-test.log`.

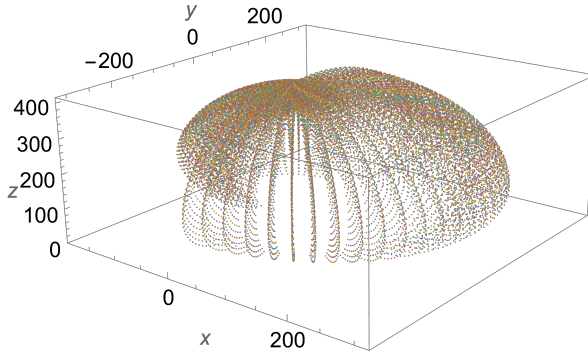


FIGURE 3. Positions of the end-effector of the EV3 manipulator for $\theta_1, \theta_4, \theta_7 \in \{-1.5, -1.4, \dots, 1.5\}$.

[8] showing that it was efficient and stable for solving systems of polynomial equations that were similar to the present ones.

In the case more than one solution of the inverse kinematic problem is found, the program returns the first one in the solution set (see Section 7).

5. Examples of the inverse kinematic computation

We demonstrate examples of the inverse kinematic computation¹⁶.

To obtain ideas on the feasible region of the EV3 manipulator, We have plotted positions of the end-effector for given configuration of the joints with Mathematica¹⁷. Figure 3 shows the positions of the end-effector in the \mathbb{R}^3 space for $\theta_1, \theta_4, \theta_7 \in \{-1.5(\simeq \pi/2), -1.4, \dots, 1.5(\simeq \pi/2)\}$ and Figure 4 shows them for $\theta_1 = 0$ and $\theta_4, \theta_7 \in \{-1.5, -1.4, \dots, 1.5\}$ on the xz -plane. Note that the plotted points do not necessarily guarantee that they do not overlap with other components of the robot such as the pedestal or the Intelligent Brick: in such a case, the range of the motion of the corresponding joint must be reduced.

Since we have $V_{\mathbb{C}}(I_{33,1}) = V_{\mathbb{C}}(\{0\}) = \mathbb{C}^3$, we expect that most of the given point $(x, y, z) \in \mathbb{R}^3$ belongs to segment \mathcal{S}_{33} . For example, for $(x_1, y_1, z_1) = (-6061/41, -7679/51, 4379/27)$, the solver calculates that $(x_1, y_1, z_1) \in \mathcal{S}_{33}$. Then, the solver calculates that the system of polynomial equations has

¹⁶The examples were calculated with Risa/Asir with the program file `main-steps/present-method/cgs-qe-ik-example.py` and the log file `main-steps/present-method/log/cgs-qe-ik-example.log`.

¹⁷The computation is saved in a Mathematica notebook file `main-steps/present-method/ev3-feasible-region.nb`.

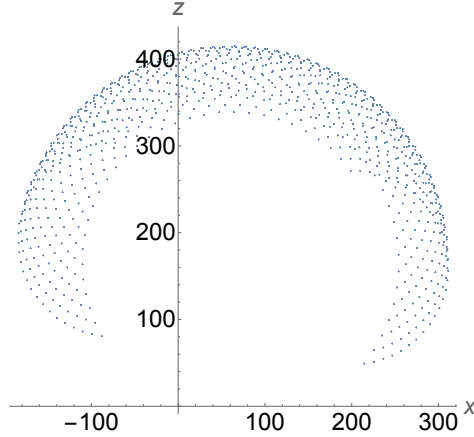


FIGURE 4. Positions of the end-effector of the EV3 manipulator for $\theta_1 = 0$, $\theta_4, \theta_7 \in \{-1.5, -1.4, \dots, 1.5\}$.

two real roots. By solving the system of polynomial equations, the configuration of the joints is calculated as

$$\begin{aligned} &(\theta_1, \theta_4, \theta_7) \\ &= (0.794578128292431 - \pi, 0.859415097289073 - \pi, -1.38522249366716 + \pi), \\ &\quad (0.794578128292431 - \pi, -0.679494508722899, 1.15100500453343 - \pi). \end{aligned}$$

Points in the feasible region which do not belong to segment \mathcal{S}_{33} are those satisfying that $x = y = 0$. For example, for $(x_2, y_2, z_2) = (0, 0, 200)$, the solver calculates that $(x_2, y_2, z_2) \in \mathcal{S}_{36}$. Then, the solver calculates that the system of polynomial equations has two real roots. By solving the system of polynomial equations, the configuration of the joints is calculated as

$$\begin{aligned} &(\theta_1, \theta_4, \theta_7) = (0, 0.236922524685754, -0.658765540873251 + \pi), \\ &\quad (0, -0.997268873826373 + \pi, 0.424548051739522 - \pi). \end{aligned}$$

For a point not in the feasible region, the solver first calculates if the point belongs to a segment. If the point belongs to a segment, then the solver calculates the number of real roots of the system of polynomial equations. If the solver verifies that there exist real roots, it solves the system of polynomial equations. For example, for $(x_3, y_3, z_3) = (300, 0, 400)$, the solver calculates that $(x_3, y_3, z_3) \in \mathcal{S}_1$. Then, the solver calculates that the system of polynomial equations has no real roots, and stops the computation.

6. Experiments

We have tested our implementation along with a comparison of its performance with the previous one that we had proposed [8], by solving inverse kinematic problems with randomly given positions of the end-effector.

TABLE 2. A result of the inverse kinematics computation with real quantifier elimination.

Test	T_{Verify} (sec.)	T_{Solve} (sec.)	T_{Total} (sec.)	Error (mm)
1	0.367	0.174	0.541	1.254×10^{-9}
2	0.365	0.179	0.544	1.659×10^{-8}
3	0.370	0.177	0.548	2.172×10^{-9}
4	0.369	0.182	0.551	1.350×10^{-9}
5	0.367	0.169	0.536	2.763×10^{-9}
6	0.367	0.169	0.536	4.312×10^{-8}
7	0.367	0.169	0.536	1.873×10^{-9}
8	0.367	0.170	0.536	1.403×10^{-9}
9	0.367	0.166	0.533	1.313×10^{-9}
10	0.368	0.170	0.538	1.222×10^{-8}
Average	0.367	0.172	0.540	8.405×10^{-9}

Our experiments consist of 10 sets of tests conducted with 100 random positions of the end-effector within the feasible region of the manipulator, given in each set of experiments (thus, 1000 random points were given in total)¹⁸. The coordinates of the sample points are given as rational numbers with the magnitude of the denominator less than 100 (mm).

The computing environment is as follows (note that we have used a virtual machine on a desktop operating system).

Host environment. Intel Core i5-8259U CPU 2.30GHz, RAM 16GB, macOS 11.4, Parallels Desktop for Mac Business Edition 16.5.1.

Guest environment. RAM 2GB, Linux 4.15.0, Python 3.6.9, NumPy 1.19.5, SymPy 1.8, OpenXM 1.3.3, Risa/Asir 20210326 (Kobe Distribution).

Note that, in comparison with our previous method, we have used the model of the manipulator in the present paper.

Table 2 shows the result of experiments of Algorithm 2. In each test, T_{Verify} is the sum of computing times of Lines 1, 5 and 6, averaged over 100 examples, for verification of the existence of real roots. T_{Solve} is the sum of computing times of Lines 10 and 12, averaged over 100 examples, for solving a system of polynomial equations. T_{Total} is the average of total computing time for inverse kinematics computation, and ‘Error’ is the average of the absolute error, or the 2-norm distance of the end-effector from the randomly given position to the calculated position with the configuration of the computed joint angles $\theta_1, \theta_4, \theta_7$. The bottom row ‘Average’ shows the average values in each column of the 10 test sets.

¹⁸We have divided 1000 problems into 10 test sets, each with 100 problems because, in the experiment of our previous work [8], the computation of Risa/Asir stopped with an error when more than 100 problems were given at once. Although the cause of the error is not clear, since then, we have divided problems into sets of 100 test cases to avoid such errors.

TABLE 3. A result of the inverse kinematics computation with our previous method [8]. Note that the model of the manipulator is renewed as the one in the present paper.

Test	$T2_{\text{GB}}$ (sec.)	$T2_{\text{Solve}}$ (sec.)	$T2_{\text{Total}}$ (sec.)	Error2 (mm)
1	0.497	0.196	0.693	1.891×10^{-9}
2	0.472	0.222	0.694	2.278×10^{-9}
3	0.474	0.225	0.699	1.914×10^{-9}
4	0.451	0.245	0.696	1.947×10^{-9}
5	0.497	0.204	0.701	1.917×10^{-9}
6	0.473	0.220	0.693	1.948×10^{-9}
7	0.495	0.203	0.699	1.951×10^{-9}
8	0.474	0.223	0.698	1.969×10^{-9}
9	0.479	0.225	0.704	1.984×10^{-9}
10	0.476	0.221	0.697	2.024×10^{-9}
Average	0.479	0.219	0.697	1.982×10^{-9}

Table 3 shows the result of experiments with our previous method for comparison, with the same inputs as those shown as in Table 2. In each test, $T2_{\text{GB}}$ is the average computing time of Gröbner basis, $T2_{\text{Solve}}$ is the average computing time for solving the system of algebraic equations, $T2_{\text{Total}}$ is the average of total computing time for inverse kinematics computation, and ‘Error2’ is the average of the absolute error, or the 2-norm distance of the end-effector from the randomly given position to the calculated position with the configuration of the computed joint angles $\theta_1, \theta_4, \theta_7$.

These results show that Algorithm 2 solves the inverse kinematic problem in a smaller amount of time than the previous method, with verification of the existence of real roots. Also, in the present method, we have observed that the number of solutions of the inverse kinematic problem was 2 or 4 for the given position of the end-effector. (For further discussions, see Section 7.) As for the accuracy of the solutions, since the actual size of the manipulator is approximately 100 mm, computed solutions with the present method seem sufficiently accurate, although the average of errors in the present method is slightly larger than that in the previous method.

7. Concluding remarks

In this paper, we have presented a method and an implementation of the inverse kinematics computation of a 3 DOF robot manipulator using the CGS-QE algorithm. Our method consists of Algorithms 1 (the preprocessing steps) and 2 (the main steps). In Algorithm 1, using the CGS-QE algorithm, we choose segments in the algebraic partition that have real coordinates and calculate the characteristic polynomial of the Hermite quadratic form. In Algorithm 2, for given parameters, after verification of the existence of real roots using the results in Algorithm 1, a system of polynomial equations is

solved after substituting the parameters in a Gröbner basis in the CGS with the given values.

Compared to our previous method, we see that the present method solves the inverse kinematic problem with the solutions as accurate as those solved with the previous method. Furthermore, the present method has the following benefits.

1. With verification of the existence of real roots using the CGS-QE algorithm, one can judge the existence of the solution to the inverse kinematic problem. Furthermore, if the given position of the end-effector is not feasible, one can avoid the useless computation of solving polynomial equations.
2. The system of polynomial equations to be solved is constructed just by substituting parameters in the corresponding Gröbner basis with the given position of the end-effector; it avoids the iterative computation of Gröbner basis for each given value.

Experimental results show that Algorithm 2 in the present method solve the inverse kinematic problem more efficiently than our previous method. However, in the present method, one also needs time for executing Algorithm 1. Thus, the previous method might be more efficient for those who build an inverse kinematic solver from scratch for solving the inverse kinematic problem for just one choice of parameters. On the other hand, in other cases, such as using a pre-built solver only with Algorithm 2 or solving the inverse kinematic problem (with Algorithm 1) for many choices of parameters, the present method will be more desirable. Furthermore, it will be preferable to automate the execution of Algorithm 1, and finding a threshold number of choice of parameters where the present method overwhelm (including the time for executing Algorithm 1) over the previous method will be one of our next tasks.

Other rooms for improvements on the present method or future research directions include(s) the following.

1. If more than one solution of the inverse kinematic problem exists, we choose the first one in the list of solutions in our current implementation. However, it is desirable to choose an appropriate one based on certain criteria such as the *manipulability measure* [24] which indicates how the current configuration of the manipulator is away from a singular configuration.
2. Experimental results show that the number of roots of the inverse kinematic problem varies with the given position of the end-effector. Analyzing how the number of roots changes in the feasible region will be preferable for choosing an appropriate one and understanding the problem's characteristics, such as kinematic singularities.
3. The quantified formula (4) we consider in this paper is a fully existentially quantified formula, thus a satisfiable modulo theory (SMT) solver such as Z3 [5] might be useful for quantifier elimination.

4. We still use Mathematica in Algorithm 1, despite our aim to use free software for building a solver. Although it is no problem to use only Algorithm 2 with a pre-built solver which incorporates only free software, building an implementation of Algorithm 1 with free computer algebra systems (such as SymPy or Z3 simplifier) is desired to achieve our goals.
5. Although, our computation of CGS in Algorithm 1 (see Section 3), an order of the variables was given as in Equation (11), any other order can be used. It would be interesting to observe how the change of order of the variables affects the result or the performance of the algorithm.
6. In the experiments, further investigation will be needed to determine a reason for higher errors in the solutions in the present method, although their magnitude seems sufficiently small compared to the required accuracy of the solutions. We know that terms appearing in the system of polynomial equations in the present method is different from those in the previous method: in the previous method, the system of polynomial equations is given as

$$\begin{aligned}
 g_1(s_7) &= s_7^4 + r_1(s_7) = 0, & g_2(c_7, s_7) &= c_7 + r_2(s_7) = 0, \\
 g_3(s_4, s_7) &= s_4 + r_3(s_7) = 0, & g_4(c_4, s_7) &= c_4 + r_4(s_7) = 0, \\
 g_5(s_1, s_7) &= s_1 + r_5(s_7) = 0, & g_6(c_1, s_7) &= c_1 + r_6(s_7) = 0,
 \end{aligned}$$

where $r_i(s_7)$ ($i = 1, \dots, 6$) is a univariate polynomial in s_7 of degree 3. On the other hand, in the present method, the system of polynomial equations is given as in Section 4.4.2, in which it seems that the polynomials are slightly complicated (some polynomials have more number of variables in them) than those in the previous method, which might affect the errors in the solution.

For our future research, applying the present method to inverse kinematics of more complicated forms (such as more degree of freedom) might be interesting. Also, solving quantified formulas with inequality or inequation constraints is expected to have a positive effect on the practicality of the present method.

References

- [1] E. Becker and T. Wörmann. On the trace formula for quadratic forms. In *Recent advances in real algebraic geometry and quadratic forms (Berkeley, CA, 1990/1991; San Francisco, CA, 1991)*, volume 155 of *Contemp. Math.*, pages 271–291. Amer. Math. Soc., Providence, RI, 1994.
- [2] D. Chablat, G. Moroz, F. Rouillier, and P. Wenger. Using maple to analyse parallel robots. In J. Gerhard and I. Kotsireas, editors, *Maple in Mathematics Education and Research*, pages 50–64, Cham, 2020. Springer International Publishing.
- [3] D. A. Cox, J. Little, and D. O’Shea. *Using Algebraic Geometry*. Springer, 2nd edition, 2005.

- [4] D. A. Cox, J. Little, and D. O’Shea. *Ideals, Varieties, and Algorithms: An Introduction to Computational Algebraic Geometry and Commutative Algebra*. Springer, 4th edition, 2015.
- [5] L. de Moura and N. Bjørner. Z3: An efficient smt solver. In C. R. Ramakrishnan and J. Rehof, editors, *Tools and Algorithms for the Construction and Analysis of Systems*, pages 337–340. Springer, 2008.
- [6] J.-C. Faugère, J.-P. Merlet, and F. Rouillier. On solving the direct kinematics problem for parallel robots. Research Report RR-5923, INRIA, 2006.
- [7] R. Fukasaku, H. Iwane, and Y. Sato. Real Quantifier Elimination by Computation of Comprehensive Gröbner Systems. In *Proceedings of the 2015 ACM on International Symposium on Symbolic and Algebraic Computation, ISSAC ’15*, page 173–180, New York, NY, USA, 2015. Association for Computing Machinery.
- [8] N. Horigome, A. Terui, and M. Mikawa. A Design and an Implementation of an Inverse Kinematics Computation in Robotics Using Gröbner Bases. In A. M. Bigatti, J. Carette, J. H. Davenport, M. Joswig, and T. de Wolff, editors, *Mathematical Software – ICMS 2020*, pages 3–13, Cham, 2020. Springer International Publishing.
- [9] C. M. Kalker-Kalkman. An implementation of Buchbergers’ algorithm with applications to robotics. *Mech. Mach. Theory*, 28(4):523–537, 1993.
- [10] D. Kapur, Y. Sun, and D. Wang. A new algorithm for computing comprehensive gröbner systems. In *Proceedings of the 2010 International Symposium on Symbolic and Algebraic Computation, ISSAC ’10*, page 29–36, New York, NY, USA, 2010. Association for Computing Machinery.
- [11] H. Kawasaki and T. Shimizu. Development of robot symbolic analysis system: ROSAM II (in Japanese). *Journal of the Robotics Society of Japan*, 17(3):408–415, 1999.
- [12] A. Koubaa, editor. *Robot Operating System (ROS): The Complete Reference*, volume 1–4. Springer, 2016–2020.
- [13] M. Maekawa, M. Noro, K. Ohara, N. Takayama, and K. Tamura. The design and implementation of OpenXM-RFC 100 and 101. In K. Shirayanagi and K. Yokoyama, editors, *Computer Mathematics: Proceedings of the Fifth Asian Symposium on Computer Mathematics (ASCM 2001)*, pages 102–111. World Scientific, 2001.
- [14] A. Meurer, C. P. Smith, M. Paprocki, O. Čertík, S. B. Kirpichev, M. Rocklin, A. Kumar, S. Ivanov, J. K. Moore, S. Singh, T. Rathnayake, S. Vig, B. E. Granger, R. P. Muller, F. Bonazzi, H. Gupta, S. Vats, F. Johansson, F. Pedregosa, M. J. Curry, A. R. Terrel, Š. Roučka, A. Saboo, I. Fernando, S. Kulal, R. Cimrman, and A. Scopatz. SymPy: symbolic computing in Python. *PeerJ Computer Science*, 3, 2017.
- [15] A. Montes. *The Gröbner Cover*. Springer, 2018.
- [16] K. Nabeshima. CGS: a program for computing comprehensive Gröbner systems in a polynomial ring [computer software], 2018. <https://www.rs.tus.ac.jp/~nabeshima/software.html> (Accessed 2021-10-24).
- [17] J. Nethery and M. Spong. Robotica: a Mathematica package for robot analysis. *IEEE Robotics & Automation Magazine*, 1(1):13–20, 1994.

- [18] M. Noro. A computer algebra system: Risa/Asir. In M. Joswig and N. Takayama, editors, *Algebra, Geometry and Software Systems*, pages 147–162. Springer, 2003.
- [19] OpenXM Committers. Risa/Asir (Kobe Distribution) [computer software]. <http://www.math.kobe-u.ac.jp/Asir/> (Accessed 2021-10-24).
- [20] OpenXM Committers. OpenXM, a project to integrate mathematical software systems [computer software], 1998–2021. <http://www.openxm.org/> (Accessed 2021-10-24).
- [21] P. Pedersen, M.-F. Roy, and A. Szpirglas. Counting real zeros in the multivariate case. In *Computational algebraic geometry (Nice, 1992)*, volume 109 of *Progr. Math.*, pages 203–224. Birkhäuser Boston, Boston, MA, 1993.
- [22] J. Pitt, D. Hildenbrand, M. Stelzer, and A. Koch. Inverse kinematics of a humanoid robot based on conformal geometric algebra using optimized code generation. In *Humanoids 2008 — 8th IEEE-RAS International Conference on Humanoid Robots*, pages 681–686, 2008.
- [23] B. Siciliano and O. Khatib, editors. *Springer Handbook of Robotics*. Springer, 2008.
- [24] B. Siciliano, L. Sciavicco, L. Villani, and G. Oriolo. *Robotics: Modelling, Planning and Control*. Springer, 2008.
- [25] A. Suzuki and Y. Sato. A simple algorithm to compute comprehensive Gröbner bases using Gröbner bases. In *Proceedings of the 2006 International Symposium on Symbolic and Algebraic Computation*, ISSAC '06, page 326–331, New York, NY, USA, 2006. Association for Computing Machinery.
- [26] A. Terui, S. Otaki, and M. Mikawa. ev3-cgs-qe-ik: An inverse kinematics solver based on the CGS-QE algorithm for an EV3 manipulator [computer software], 2021. <https://doi.org/10.5281/zenodo.5594896>.
- [27] T. Uchida and J. McPhee. Triangularizing kinematic constraint equations using Gröbner bases for real-time dynamic simulation. *Multibody System Dynamics*, 25:335–356, 2011.
- [28] T. Uchida and J. McPhee. Using Gröbner bases to generate efficient kinematic solutions for the dynamic simulation of multi-loop mechanisms. *Mech. Mach. Theory*, 52:144–157, 2012.
- [29] S. van der Walt, S. C. Colbert, and G. Varoquaux. The NumPy Array: A Structure for Efficient Numerical Computation. *Comput. Sci. Eng.*, 13(2):22–30, 2011.
- [30] K. Waldron and J. Schmiedeler. Kinematics. in [23], pages 9–34.
- [31] J. Wallén. On robot modelling using Maple. Technical Report, Linköping University, 2007.
- [32] V. Weispfenning. A new approach to quantifier elimination for real algebra. In B. F. Caviness and J. R. Johnson, editors, *Quantifier Elimination and Cylindrical Algebraic Decomposition*, pages 376–392, Vienna, 1998. Springer Vienna.

Shuto Otaki
Graduate School of Pure and Applied Sciences
University of Tsukuba
Tsukuba-shi, Ibaraki 305-8571
Japan
Current affiliation:
Tokiwa Senior High School
Ota-shi, Gunma 373-0817
Japan
e-mail: otakishuto@math.tsukuba.ac.jp

Akira Terui
Faculty of Pure and Applied Sciences
University of Tsukuba
Tsukuba-shi, Ibaraki 305-8571
Japan
e-mail: terui@math.tsukuba.ac.jp

Masahiko Mikawa
Faculty of Library, Information and Media Science
University of Tsukuba
Tsukuba-shi, Ibaraki 305-8550
Japan
e-mail: mikawa@slis.tsukuba.ac.jp